Manuscript submitted to
AIMS' Journals
Volume **X**, Number **0X**, XX **200X**

doi:10.3934/xx.xx.xx.xx

pp. **X–XX**

PHLST WITH ADAPTIVE TILING AND ITS APPLICATION TO ANTARCTIC REMOTE SENSING IMAGE APPROXIMATION

Zhihua Zhang

College of Global Change and Earth System Science, Beijing Normal University
Beijing, China, 100875

Naoki Saito

Department of Mathematics, University of California
Davis, California, 95616, USA

(Communicated by the associate editor name)

Abstract. We propose an efficient nonlinear approximation scheme using the Polyharmonic Local Sine Transform (PHLST) of Saito and Remy combined with an algorithm to tile a given image automatically and adaptively according to its local smoothness and singularities. To measure such local smoothness, we introduce the so-called local Besov indices of an image, which is based on the pointwise modulus of smoothness of the image. Such an adaptive tiling of an image is important for image approximation using PHLST because PHLST stores the corner and boundary information of each tile and consequently it is wasteful to divide a smooth region of a given image into a set of smaller tiles. We demonstrate the superiority of the proposed algorithm using Antarctic remote sensing images over the PHLST using the uniform tiling. Analysis of such images including their efficient approximation and compression has gained its importance due to the global climate change.

1. **Introduction.** In 2006, Saito and Remy [11] introduced a new tool for image analysis and synthesis, which is named *Polyharmonic Local Sine Transform* (PHLST). The PHLST resolves several problems occurring in the Local Trigonometric Transforms (LTTs) of Coifman and Meyer [5] and Malvar [9, 8], such as the overlapping windows and the slopes of the bell functions. PHLST first segments (or more precisely "tiles") an image into local pieces (i.e., blocks) using the characteristic functions, then decomposes each piece into two components: the *polyharmonic component* and the *residual*. The polyharmonic component is obtained by solving the elliptic boundary value problem associated with the so-called polyharmonic equation (e.g., Laplace's equation, biharmonic equation, etc.) given the boundary values (the pixel values along the boundary created by the characteristic function).

2010 *Mathematics Subject Classification.* Primary: 42C40, 65D18; Secondary: 68W25.

Key words and phrases. PHLST, adaptive tiling, Antarctic remote sensing, image approximation, climate change.

The first author was partially supported by National Key Science Program for Global Change Research No.2013CB956604 and No.2010CB950504; Fundamental Research Funds for the Central Universities (Key Program) No.105565GK; the Scientific Research Foundation for the Returned Overseas Chinese Scholars, State Education Ministry; and Polar Climate and Environment Key Laboratory. The second author was partially supported by ONR grants: N00014-09-1-0041, N00014-09-1-0318, N00014-12-1-0117.

Subsequently this component is subtracted from the original local piece to obtain the residual. Since the boundary values of the residual vanish, its Fourier sine series expansion has quickly decaying coefficients. Consequently, PHLST can distinguish *intrinsic* singularities in the data from the artificial discontinuities created by the local windowing. Combining this ability with the quickly decaying coefficients of the residuals, PHLST is also effective for image approximation, which was demonstrated using both synthetic and real images in [11]. Of critical importance in PHLST is how to tile an input image. As discussed in [11], there is no need to divide a smooth region of a given image into a set of smaller blocks, and in fact, that is wasteful due to the storage of the corner and boundary information in each block. In [11], however, Saito and Remy did not propose any automatic tiling algorithm for PHLST. In this paper, we will propose the PHLST equipped with an adaptive tiling algorithm for efficiently approximating given input images. We will demonstrate the effectiveness of the PHLST with the adaptive tiling algorithm for approximating Antarctic remote sensing images. Since such remote sensing images often consists of a large smooth part and smaller singular regions represented by snow ripples, fractured ice, and coastlines, our proposed PHLST algorithm is more effective to approximate such images then the PHLST with the uniform tiling as was done in [11].

We also would like to mention the importance of efficiently approximating and compressing such Antarctic remote sensing images. The current world is facing a series of unprecedented major global environmental problems caused by global warming. In the 2007 Fourth Assessment Report (AR4) by the Intergovernmental Panel on Climate Change (IPCC) of the United Nations, it is indicated that most of the observed warming over the last 50 years is likely to have been due to the increasing concentrations of greenhouse gases produced by human activities such as deforestation and burning fossil fuel. In polar regions, warming will be expected to be strongest and cause the retreat of glaciers and sea ices, even the melting of ice sheets. Partial deglaciation of the West Antarctic ice sheet could contribute 4-6 meters or more to sea level rise. This will be a big disaster for human being. A good approach to observe and analyze the change of ice structures is to compare remote sensing images of Antarctica taken at difference times. Such an endeavor forces one to store a huge amount of remote sensing data. In order to save storage space, one needs to develop a new image compression algorithm that can efficiently preserve intrinsic features (or singularities) of Antarctic remote sensing images with small storage costs.

This paper is organized as follows. In Section 2, we recall the concept of PHLST. In Section 3, in order to measure the local smoothness of an image, we introduce the concept of local Besov indices and discuss the relation between local Besov indices and global Besov indices. Based on these indices, in Section 4, we derive a fundamental principle of adaptive tiling. In Section 5, we obtain a precise estimate of the nonlinear approximation error of the target function using PHLST with adaptive tiling. It is clear that the obtained nonlinear approximation order using PHLST with adaptive tiling is much better than that using PHLST with uniform tiling. In Section 6, we apply our research on nonlinear approximation using PHLST with adaptive tiling to Antarctic remote sensing image approximation.

2. **Polyharmonic local sine transform.** A function f supported on a cube Ω is divided into a set of functions on subcubes using the characteristic functions

$$\Omega = \bigcup_{j=1}^{J} \Omega_j \quad \text{and} \quad f_j = f\chi_{\Omega_j},$$

and then split each piece f_j in two components: the polyharmonic component u_j and the residual v_j, i.e., $f_j = u_j + v_j$. Let Δ be the Laplace operator in $\mathbb{R}^d$, i.e.,

$$\Delta = \frac{\partial^2}{\partial x_1^2} + \frac{\partial^2}{\partial x_2^2} + \cdots + \frac{\partial^2}{\partial x_d^2}.$$

Then the polyharmonic component u_j is the solution of the following polyharmonic equation, i.e.,

$$\Delta^m u_j = 0 \quad \text{in } \Omega_j \text{ for some } m \in \mathbb{N} \tag{1}$$

with boundary conditions

$$\frac{\partial^{2l} u_j}{\partial \nu^{2l}} = \frac{\partial^{2l} f_j}{\partial \nu^{2l}} \quad \text{on } \partial\Omega_j \qquad (l = 0, ..., m-1), \tag{2}$$

where $\frac{\partial^{2l}}{\partial \nu^{2l}}$ is the normal derivative at the boundary. Subtracting u_j from f_j, we get the residual v_j. We do odd extension of v_j followed by its periodic extension to extend v_j from Ω_j to $\mathbb{R}^d$. Denote the obtained function by v_j^*. We expand v_j^* into the Fourier sine series. The Fourier sine expansion coefficients of v_j^* decay rapidly if there is no intrinsic singularity in f_j. This process is called the *Polyharmonic Local Sine Transform* (PHLST) [11].

In image compression and approximation, as long as the boundary data are stored and the normal derivatives at the boundary are available, the polyharmonic components can be computed quickly by utilizing the FFT-based Laplace solver developed by Averbuch, Braverman, Israeli, and Vozovoi [1, 2], which we shall call the ABIV method. Moreover, the FFT-based Discrete Sine Transform is used to generate the Fourier sine coefficients of the residuals. Hence the PHLST is a fast algorithm with its computational cost $O(n \log n)$ where n is a number of pixels in an image.

When $m = 1$, (1) and (2) are reduced to

$$\Delta u_j = 0 \text{ in } \Omega_j \quad \text{and} \quad v_j = 0 \text{ on } \partial\Omega_j,$$

the corresponding algorithm is called the *Laplace Local Sine Transform* (LLST).

In particular, for $d = 2$, $m = 1$, f is a bivariate function and each Ω_j is a square and $\Delta = \frac{\partial^2}{\partial x_1^2} + \frac{\partial^2}{\partial x_2^2}$. For $d = 1$, $m \in \mathbb{N}$, f is a univariate function, $\Delta^m = \frac{\partial^{2m}}{\partial x_1^{2m}}$, each Ω_j is a closed interval $[a_j, b_j]$, and $\partial\Omega_j$ are the endpoints a_j and b_j. Hence u_j becomes a polynomial of degree $2m - 1$.

3. **Besov space and Local Besov indices.** We use the Besov space as the measure of the smoothness of a target function. To reflect the smoothness at each point, we introduce the concept of local Besov indices and explain the relation between the local Besov index at each point and the global Besov index. Based on these indices, in Section 4, we derive a fundamental principle of adaptive tiling.

The definition of the Besov space is based on the notion of moduli of smoothness. Let Ω be a domain in $\mathbb{R}^d$ and a target function $f \in L^p(\Omega)\,(1 \le p < \infty)$. Denote the

rth difference with step h by $\Delta_h^r(f;x)$:

$$\Delta_h^r(f;x) := \sum_{\nu=0}^{r}(-1)^{r-\nu}\, C_r^\nu\, f(x+\nu h) \qquad \left(C_r^\nu = \frac{r!}{(r-\nu)!\nu!}\right).$$

The *modulus of smoothness* of f in $L^p(\Omega)\,(1 \le p < \infty)$ is defined as

$$\omega_r(f,t)_p := \sup_{|h|<t} \|\Delta_h^r(f;x)\|_{L^p(\Omega)}.$$

For $\alpha > 0$, *Besov spaces* are defined as

$$B^\alpha(L^p(\Omega)) := \{\, f \in L^p(\Omega), \quad \omega_r(f;\ t)_p = O(t^\alpha)\,\},$$

where r is the smallest integer larger than α.

Let Ω be a bounded domain of $\mathbb{R}^d$ and $f \in L^p(\Omega)$ $(1 \le p \le \infty)$. Now we define the *global Besov index* on the domain Ω.

Definition 3.1. We define the *global Besov index* of f on the domain Ω as follows:

$$\alpha_f(\Omega) := \sup\{\alpha > 0 \,|\, f \in B^\alpha(L^p(\Omega))\}.$$

We define local Besov indices as follows.

Definition 3.2. Let $f \in L^p(\Omega)$ $(1 \le p \le \infty)$ and $x \in \Omega$. Denote the ball with the center x and radius δ by $B_\delta(x)$ and $D_\delta(x) := B_\delta(x) \cap \Omega$. Define

$$\alpha_f(x) = \sup_{\delta>0}\{\alpha_f(D_\delta(x))\}$$

and call $\alpha_f(x)$ the *local Besov index* of f at the point x.

The following theorem explains the relations between global and local Besov indices.

Theorem 3.3. *Let Ω be a domain of $\mathbb{R}^d$ and $f \in L^p(\Omega)$. Then we have*

$$\alpha_f(\Omega) = \inf_{x\in\Omega} \alpha_f(x), \tag{3}$$

where $\alpha_f(\Omega)$ and $\alpha_f(x)$ are the global Besov index and the local Besov index of f at the point x, respectively.

Proof. Let $\alpha = \inf_{x\in\Omega} \alpha_f(x)$. Clearly, we have $\alpha_f(x) \ge \alpha$. By Definition 3.2, for $x \in \Omega$ and $\lambda > 0$, there exists a $\delta(x) > 0$ such that

$$\alpha_f(D_{\delta(x)}(x)) > \alpha_f(x) - \lambda \ge \alpha - \lambda \qquad (x \in \Omega).$$

By Definition 3.1, we have

$$f\chi_{D_{\delta(x)}(x)} \in B^{\alpha-\lambda}(L^p(D_{\delta(x)}(x))), \tag{4}$$

where χ_E is the characteristic function of the set E. Since the system of open balls $\{D_{\delta(x)}(x)\}_{x\in\Omega}$ covers the bounded closed domain Ω, by the theorem of finite covering, we know that there exists a system of finitely many open balls $\{D_{\delta(x_l)}(x_l)\}_{l=1}^L$ which covers the closed domain Ω.

Let $f_l^* = f\chi_{D_{\delta(x_l)}(x_l)}$. By (4), we have

$$f_l^* \in B^{\alpha-\lambda}(L^p(D_{\delta(x_l)}(x_l))) \qquad (l = 1, ..., L). \tag{5}$$

Let Ω_1, Ω_2 and $\Omega_1 \cup \Omega_2$ be both domains. By the definition of the Besov space, we know that the following claim:

"If $\quad f \in B^s(L^p(\Omega_1))\quad$ and $\quad f \in B^s(L^p(\Omega_2)),\quad$ then $\quad f \in B^s(L^p(\Omega_1 \cup \Omega_2))$."

holds.

Since $\bigcup_{l=1}^{L} B_{\delta(x_l)}(x_l) \supset \Omega$ and $\bigcup_{l=1}^{L} B_{\delta(x_l)}(x_l)$ is a domain, using the above claim together with (5), we have $f \in B^{\alpha-\lambda}(L^p(\Omega))$. Since λ is arbitrarily small, by Definition 3.1, it follows that

$$\alpha_f(\Omega) \geq \alpha. \tag{6}$$

On the other hand, by Definitions 3.1 and 3.2, we easily see that $\alpha_f(x) \geq \alpha_f(\Omega)$ for any $x \in \Omega$. So we have $\alpha = \inf_{x\in\Omega} \alpha_f(x) \geq \alpha_f(\Omega)$. From this and (6), we get (3). □

4. **Adaptive tiling.** In this section, using local Besov indices, we will derive a fundamental principle of adaptive tiling.

Let Ω be a domain in $\mathbb{R}^2$ and the target function $f \in L^p(\Omega)\,(2 \leq p < \infty)$. Using the local Besov index of f at every point in Ω, we may adaptively segment the domain Ω and the function f.

Let ε be a given approximation error. Since $f \in L^p(\Omega)$, by the absolute continuity of integral, for the given $\varepsilon > 0$, there exists a $\eta > 0$ such that for any set $F \subset \Omega$ whose measure $|F| \leq \eta$, we have

$$\|f\chi_F\|_{L^p(\Omega)} = \left(\int_F |f|^p \, \mathrm{d}x \right)^{\frac{1}{p}} \leq \frac{\varepsilon}{2}. \tag{7}$$

From this, we see that deleting a non-smooth part with small measure does not affect image approximation too much. More precisely, for the above $\eta > 0$, we can choose a set E and an index $\alpha_0 > 0$ such that

$$|E| < \eta, \qquad \sup_{x\in E} \alpha_f(x) < \alpha_0, \qquad \alpha_f(x) \geq \alpha_0 \quad (x \in \Omega \setminus E).$$

Below we give an adaptive tiling of the domain Ω based on the above set E

We choose two sets of squares A and B step by step, where A is a set of 'good' squares and B is a set of 'bad' squares as follows.

Step 1. We divide the domain Ω into four squares $\{\Omega_j\}_1^4$:

$$\Omega = \bigcup_{j=1}^{4} \Omega_j,$$

where Ω_j are pairwise disjoint except their boundaries. Initially, we set the "good set" A as an empty set and the " bad set " B as a set of all four squares, i.e.,

$$A = \emptyset \quad \text{and} \quad B = \{\Omega_j\}_1^4.$$

Step 2. Let Ω_j be a square in the bad set B. If Ω_j does not intersect with E, i.e., $\Omega_j \cap E = \emptyset$, then we call this square Ω_j a "good square". We remove this good square from the bad set B and add it to the good set A. Denote

$$A := \{\Omega_k^*\}.$$

If Ω_j intersects with E, i.e., $\Omega_j \cap E \neq \emptyset$, then we call Ω_j is a "bad square". We retain the "bad square" in the bad set B. Denote

$$B := \{\Omega_k^{**}\}.$$

Step 3. If the sum of the measures of squares in B is larger than η:

$$\sum |\Omega_k^{**}| > \eta,$$

where η is stated as above, then we return Steps 1 and 2. We divide Ω_k^{**} into four squares $\{\Omega_{k,l}^{**}\}_{l=1}^4$.

For each square $\Omega_{k,l}^{**}$,

(i) if $\Omega_{k,l}^{**} \cap E = \emptyset$, then we call $\Omega_{k,l}^{**}$ is a " good square ". We remove this " good square " from B and add it to A;

(ii) if $\Omega_{k,l}^{**} \cap E \neq \emptyset$, then we call $\Omega_{k,l}^{**}$ is a " bad square ". We retain this " bad square " in B.

Since, in each step, $B \supset E$ and $|E| < \eta$, we may continue this procedure until the sum of measures of squares in B is less than η. We denote the final set of good squares by $A := \{Q_k\}_1^M$. Denoting $Q := \bigcup_{k=1}^{M} Q_k$, we have $|\Omega \backslash Q| = |B| < \eta$. By (7), we get

$$\|f\chi_{\Omega\backslash Q}\|_{L^p(\Omega)} = \left(\int\limits_{\Omega\backslash Q} |f|^p \, \mathrm{d}x \, \mathrm{d}y \right)^{\frac{1}{p}} \leq \frac{\varepsilon}{2}. \tag{8}$$

Since we consider the L^p-approximation of bounded functions and the values of the integrals of bounded functions on sets with small measure are small, we may delete the set $\Omega \setminus Q$ with measure $\leq \eta$ and the approximation error makes a slight change as in (8). Therefore,

$$\Omega \simeq \bigcup_{k=1}^{M} Q_k.$$

is a desired tiling of Ω.

5. L^p **approximation order.** In this section, based on the above adaptive tiling, we derive the L^p approximation orders of target functions on the domains by a combination of polyharmonic functions and sine polynomials.

Let a bivariate function $f \in L^p(\Omega)$ $(2 \leq p < \infty)$ and Ω be a bounded domain in $\mathbb{R}^2$. Using the adaptive tiling in Section 4, we obtain $Q = \bigcup_{k=1}^{M} Q_k$ and $|\Omega \setminus Q| \leq \eta$. Here $\{Q_k\}_1^M$ are disjoint squares. From (8), we know that

$$\|f\chi_{\Omega\backslash Q}\|_{L^p(\Omega)} \leq \frac{\varepsilon}{2}.$$

The approximation of the non-smooth function f on the domain Ω is reduced to the approximation of the smooth functions f on Q.

Denote the global Besov index of f on Q_k by $\alpha_k = \alpha_f(Q_k)$ $(k = 1, 2, ..., M)$ and

$$\alpha_{k_0} := \min\{\alpha_1, ..., \alpha_M\}. \tag{9}$$

We will show that the approximation order of f is determined by the minimal index α_{k_0}.

For each Q_k, using PHLST, we decompose the bivariate function f as follows

$$f\chi_{Q_k} = u_k + v_k$$

where u_k is the polyharmonic component satisfying $\Delta^{m_k} u_k = 0$ on Q_k with boundary conditions

$$\frac{\partial^{2l} u_k}{\partial \nu^{2l}} = \frac{\partial^{2l} f\,\chi_{Q_k}}{\partial \nu^{2l}} \qquad \text{on} \quad \partial Q_k \ \ (l = 0, ..., m_k - 1).$$

Here we choose m_k as large as possible, i.e., m_k is a maximal integer satisfying $2m-1 \le \alpha_k$, and v_k is the residual. Let

$$U(x) = \sum_{k=1}^{M} u_k(x)\chi_{Q_k}(x), \qquad V(x) = \sum_{k=1}^{M} v_k(x)\chi_{Q_k}(x) \tag{10}$$

Then we have

$$f(x)\chi_Q(x) = U(x) + V(x) \qquad (x \in Q), \quad \text{where} \quad Q = \bigcup_{k=1}^{M} Q_k.$$

Below we discuss approximations of $V(x)$ and $U(x)$, respectively.

5.1. **Approximation of $V(x)$.** From $\alpha_f(Q_k) = \alpha_k$, it follows that $\alpha_{v_k}(Q_k) = \alpha_k$. Therefore, for an arbitrary small positive number s,

$$v_k \in B^{\alpha_k - s}(Q_k) \quad (s > 0)$$

and

$$\frac{\partial^{2l} v_k}{\partial \nu^{2l}} = 0 \quad \text{on} \quad \partial Q_k \quad (l = 0, ..., m_k - 1).$$

Let v_k^* be the periodic odd extension of v_k. This implies that $v_k^* \in B_*^{\alpha_k - s}$, where $B_*^{\alpha_k - s}$ is periodic Besov space.

Suppose that the center of the square Q_k is $\theta_k = (\theta_1^k, \theta_2^k)$ and the length of its side is l_k. Let the space $\sum_\tau$ consist of all sine polynomials t_τ which can be expressed as

$$t_\tau(x) = \sum_{\nu \in \Lambda} \beta_\nu \sin \frac{\pi \nu_1 (x_1 - \theta_1^k)}{l_k} \sin \frac{\pi \nu_2 (x_2 - \theta_2^k)}{l_k} \qquad (x = (x_1, x_2)),$$

where each β_ν is a constant and $\Lambda \subset \mathbb{N}^2$ is a set of the cardinality $\le \tau$.

Let $\sigma_\tau(v_k^*;\ x)$ be the best approximation sine polynomial of v_k^* in the space $\sum_\tau$. We construct piecewise sine polynomials

$$V_n(x) = \sum_{k=1}^{M} \sigma_{n_k}(v_k^*; x)\chi_{Q_k}(x), \tag{11}$$

where $n = \sum_{k=1}^{M} n_k$. We will choose $n_1, ..., n_M$ such that $\|V - V_n\|_{L^p(Q)} \le \frac{\varepsilon}{4}$ and $n = n_1 + \cdots + n_M$ is small as possible. For this purpose, we choose n_k such that

$$\|\sigma_{n_k}(v_k^*) - v_k^*\|_{L^p(Q_k)} \le \frac{\varepsilon}{4M}. \tag{12}$$

By a known formula [4] of trigonometric approximation, we have

$$\|\sigma_{n_k}(v_k^*) - v_k^*\|_{L^p(Q_k)} \le C_k n_k^{-\frac{\alpha_k}{2} + s' + \frac{1}{p} - \frac{1}{2}} \qquad (s' > 0).$$

where C_k is a constant. From this, we know that (12) holds if

$$C_k n_k^{-\frac{\alpha_k}{2} + s' + \frac{1}{p} - \frac{1}{2}} \le \frac{\varepsilon}{4M}$$

i.e., we should choose that

$$n_k \approx \left(\frac{4C_k M}{\varepsilon} \right)^{\left(\frac{\alpha_k}{2} - s' - \frac{1}{p} + \frac{1}{2}\right)^{-1}}. \tag{13}$$

From this, we have

Proposition 1. *For $\varepsilon > 0$, take $n = \sum_{k=1}^{M} n_k$, where n_k is stated in (13). Let $V(x)$ and $V_n(x)$ be stated in (10) and (11), respectively. Then*

$$\|V - V_n\|_{L^p(Q)} \le \frac{\varepsilon}{4}.$$

From the construction of V_n, we know that $V_n(x)$ is a piecewise sine polynomial which is determined by n coefficients. From (13), we get the approximation order of $V(x)$ by piecewise sine polynomials $V_n(x)$.

Proposition 2. *Let $V(x)$ and $V_n(x)$ be stated in (10) and (11). Then the following estimate holds:*

$$\|V - V_n\|_{L^p(Q)} = O\left(n^{-\frac{\alpha_{k_0}}{2}+s'+\frac{1}{p}-\frac{1}{2}}\right) \qquad (2 \le p < \infty),$$

where α_{k_0} is stated in (9) and $s' > 0$ is an arbitrarily small number.

Proof. By (13), we get

$$n \le \sum_{k=1}^{M} \left(\frac{4C_k M}{\varepsilon}\right)^{\left(\frac{\alpha_k}{2}-s'-\frac{1}{p}+\frac{1}{2}\right)^{-1}}.$$

By (9): $\alpha_{k_0} = \min\{\alpha_1, ..., \alpha_M\}$, we have

$$n \le \left(\frac{4}{\varepsilon}\right)^{\left(\frac{\alpha_{k_0}}{2}-s'-\frac{1}{p}+\frac{1}{2}\right)^{-1}} \sum_{k=1}^{M} \left((C_k M)^{\left(\frac{\alpha_k}{2}-s'-\frac{1}{p}+\frac{1}{2}\right)^{-1}} J_k(\varepsilon)\right), \tag{14}$$

where $J_k(\varepsilon) = \left(\frac{4}{\varepsilon}\right)^{\left(\frac{\alpha_k}{2}-s'-\frac{1}{p}+\frac{1}{2}\right)^{-1}-\left(\frac{\alpha_{k_0}}{2}-s'-\frac{1}{p}+\frac{1}{2}\right)^{-1}}$. By $p > 2$ and $0 < \alpha_{k_0} \le \alpha_k$, we have

$$\left(\frac{\alpha_k}{2} - s' - \frac{1}{p} + \frac{1}{2}\right)^{-1} - \left(\frac{\alpha_{k_0}}{2} - s' - \frac{1}{p} + \frac{1}{2}\right)^{-1} \le 0.$$

So $J_k(\varepsilon) \le 1$. From this, we get

$$\sum_{k=1}^{M} (C_k M)^{\left(\frac{\alpha_k}{2}-s'-\frac{1}{p}+\frac{1}{2}\right)^{-1}} J_k(\varepsilon) \le \sum_{k=1}^{M} (C_k M)^{\left(\frac{\alpha_k}{2}-s'-\frac{1}{p}+\frac{1}{2}\right)^{-1}} = O(1),$$

where the constant in the term "O" is independent of ε. Again, by (14),

$$n = O\left(\left(\frac{4}{\varepsilon}\right)^{\left(\frac{\alpha_{k_0}}{2}-s'-\frac{1}{p}+\frac{1}{2}\right)^{-1}}\right).$$

This implies that

$$\frac{\varepsilon}{4} = O\left(n^{-\frac{\alpha_{k_0}}{2}+s'+\frac{1}{p}-\frac{1}{2}}\right). \tag{15}$$

By (10), (11), and (12), we get

$$\|V - V_n\|_{L^p(Q)} \le \sum_{k=1}^{M} \|v_k^* - \sigma_{n_k}(v_k^*)\|_{L^p(Q_k)} \le \frac{\varepsilon}{4}.$$

From this and (15), we have

$$\|V - V_n\|_{L^p(Q)} = O\left(n^{-\frac{\alpha_{k_0}}{2}+s'+\frac{1}{p}-\frac{1}{2}}\right) \qquad (s' > 0).$$

Proposition 2 is proved. □

5.2. **Approximation of $U(x)$.** By (10), we see that the approximation of $U(x)$ is reduced to that of each u_k on the square Q_k. Each u_k satisfies that

$$\Delta^{m_k} u_k = 0 \quad \text{and} \quad u_k = f \quad \text{on } \partial Q_k,$$

where m_k is the maximal value of $m \in \mathbb{N}$ satisfying $2(m-1) \le \alpha_k$.

Let the four sides of the square Q_k are $\tau_1^{(k)}$, $\tau_2^{(k)}$, $\tau_3^{(k)}$, and $\tau_4^{(k)}$. We first consider the approximation of u_k on each side $\tau_i^{(k)}$ by a combination of a polynomial of degree $2m_k - 1$ and a sine polynomial. From $\alpha_f(Q_k) = \alpha_k$, it follows that $\alpha_f\left(\tau_i^{(k)}\right) \ge \alpha_k$. Since $f = u_k$ on $\tau_i^{(k)}$, we have

$$\alpha_{u_k}\left(\tau_i^{(k)}\right) \ge \alpha_k. \tag{16}$$

Denote the endpoints of the side $\tau_i^{(k)}$ are $a_i^{(k)}$ and $b_i^{(k)}$. For the restriction of u_k on $\tau_i^{(k)}$, we do one-dimensional PHLST decomposition

$$u_k = g_i^{(k)} + h_i^{(k)} \qquad \text{on} \quad \tau_i^{(k)}, \tag{17}$$

where $g_i^{(k)}$ is a polynomial of degree $2m_k - 1$ and $h_i^{(k)}$ vanishes on endpoints of the side $\tau_i^{(k)}$:

$$\frac{\mathrm{d}^{2l}}{\mathrm{d}x^{2l}} h_i^{(k)}(x) = 0 \qquad \text{at} \quad x = a_i^{(k)},\ b_i^{(k)} \quad \text{for } l = 0, 1, ..., m_k - 1.$$

By (16) and (17),

$$\alpha_{h_i^{(k)}}\left(\tau_i^{(k)}\right) \ge \alpha_k.$$

When we do odd extension of $h_i^{(k)}$ followed by its periodic extension, the obtained function belongs to the periodic Besov space $B_*^{\alpha_k - s}$ $(s > 0)$. Denote the trigonometric approximation of $h_i^{(k)}$ by $\sigma_{n_k'}\left(h_i^{(k)}, x\right)$. By a known result [4], we have

$$\left\| \sigma_{n_k'}\left(h_i^{(k)}; x\right) - h_i^{(k)}(x) \right\|_{C\left(\tau_i^{(k)}\right)} \le C_k' (n_k')^{-\alpha_k + s - \frac{1}{2}}, \quad s > 0. \tag{18}$$

We choose n_k' such that

$$\left\| \sigma_{n_k'}\left(h_i^{(k)},\ x\right) - h_i^{(k)}(x) \right\|_{C\left(\tau_i^{(k)}\right)} \le \frac{\varepsilon}{4M}.$$

Let $\widetilde{u}_{n_k'}$ satisfy that

$$\Delta^{m_k} \widetilde{u}_{n_k'} = 0 \quad \text{in } Q_k \qquad \text{and} \qquad \widetilde{u}_{n_k'} = g_i^{(k)} + \sigma_{n_k'}\left(h_i^{(k)}\right) \quad \text{on} \quad \tau_i^{(k)} \quad (i = 1, 2, 3, 4). \tag{19}$$

Here the polyharmonic function $\widetilde{u}_{n_k'}$ is determined by $8m_k$ coefficients of polynomials and $4n_k'$ coefficients of sine polynomials.

Now we estimate the difference between two m_k-fold polyharmonic functions u_k and $\widetilde{u}_{n_k}$

$$||u_k - \widetilde{u}_{n_k'}||_{L_p(Q_k)} = \left(\int_{Q_k} |u_k - \widetilde{u}_{n_k'}|^p \, \mathrm{d}x_1 \, \mathrm{d}x_2 \right)^{\frac{1}{p}} \le A_k^{\frac{1}{p}} \|u_k - \widetilde{u}_{n_k'}\|_{C(Q_k)},$$

where A_k is the area of Q_k. From this and (17)-(19), by the maximum modulus principle, we get

$$\|u_k - \widetilde{u}_{n_k}\|_{C(Q_k)} = \max_{1\le i\le 4} \|h_i^{(k)} - \sigma_{n_k}\left(h_i^{(k)}\right)\|_{C\left(\tau_i^{(k)}\right)} \le C_k' n_k^{-\alpha_k+s-\frac{1}{2}}. \tag{20}$$

From this, we have the following proposition.

Proposition 3. *Let*

$$n_k' \approx \left(\frac{4C_k' M}{\varepsilon}\right)^{\left(\alpha_k - s + \frac{1}{2}\right)^{-1}} \qquad \text{and} \qquad n' = \sum_{k=1}^{M} n_k'.$$

Denote

$$U_{n'}(x) = \sum_{k=1}^{M} \widetilde{u}_{n_k'}(x)\,\chi_{Q_k}(x).$$

Then $\|U - U_{n'}\|_{L^p(Q)} \le \frac{\varepsilon}{4}$.

Again, by (20),

$$\|u_k - \widetilde{u}_{n_k'}\|_{L^p(Q_k)} = O\left((n_k')^{-\alpha_k+s-\frac{1}{2}}\right) \qquad (k = 1, ..., M).$$

This implies the following proposition.

Proposition 4.

$$\|U - U_{n'}\|_{L^p(Q)} = O\left((n')^{-\alpha_{k_0}+s-\frac{1}{2}}\right) \qquad (s > 0).$$

By Propositions 1 and 3, we obtain

Theorem 5.1. *Suppose that* $f \in L^p(\Omega)$ $(2 \le p < \infty)$ *and* Ω *be a bounded domain in* $\mathbb{R}^2$. *For* $\varepsilon > 0$, $Q = \bigcup_{k=1}^{M} Q_k$ *is an adaptive tiling of* Ω *described in Section 4 which satisfies*

$$\|f\,\chi_{\Omega\setminus Q}\|_{L^p(\Omega)} < \frac{\varepsilon}{2}.$$

Denote the global Besov index of f *on* Q_k *by* α_k. *Let*

$$f(x) = u_k(x) + v_k(x) \qquad \text{on} \quad Q_k$$

be the m_k-*fold PHLST decomposition where* m_k *is the maximal integer satisfying* $2m - 1 \le \alpha_k$ *and denote*

$$U(x) = \sum_{k=1}^{M} u_k(x)\,\chi_{Q_k}(x), \qquad V(x) = \sum_{k=1}^{M} v_k(x)\,\chi_{Q_k}(x).$$

Set

$$n_k = \left(\frac{4C_k M}{\varepsilon}\right)^{\left(\frac{\alpha_k}{2} - s' - \frac{1}{p} + \frac{1}{2}\right)^{-1}}, \qquad n = \sum_{k=1}^{M} n_k$$

$$n_k' = \left(\frac{4C_k' M}{\varepsilon}\right)^{\left(\alpha_k - s + \frac{1}{2}\right)^{-1}}, \qquad n' = \sum_{k=1}^{M} n_k',$$

where the constants C_k *and* C_k' *are stated in* (13) *and* (18). *Denote*

$$U_{n'}(x) = \sum_{k=1}^{M} u_{n_k'}(x)\,\chi_{Q_k}(x), \qquad V_n(x) = \sum_{k=1}^{M} v_{n_k}(x)\,\chi_{Q_k}(x).$$

Then $f(x) = U(x) + V(x)$ $(x \in Q)$ *and*

$$\|U - U_{n'}\|_{L^p(Q)} \le \frac{\varepsilon}{4} \qquad \textit{and} \qquad \|V - V_n\|_{L^p(Q)} \le \frac{\varepsilon}{4}.$$

From this theorem, we see that $U_{n'}(x)$ is a combination of a piecewise polyharmonic function and a piecewise sine polynomial which is determined by $4n'$ coefficients of sine polynomials and $8m$ coefficients of polynomials where $m = \sum_{k=1}^{n} m_k$, and $V(x)$ is a piecewise sine polynomial which is determined by n coefficients of sine polynomials.

By Propositions 2 and 4, we get the estimates of approximation errors.

Theorem 5.2. *Under the assumption of Theorem 5.1, we have*

$$\|U - U_n\|_{L^p(Q)} = O\left(n^{-\alpha_{k_0}+s-\frac{1}{2}}\right),$$

$$\|V - V_n\|_{L^p(Q)} = O\left(n^{-\frac{\alpha_{k_0}}{2}+s+\frac{1}{p}-\frac{1}{2}}\right),$$

where $Q = \bigcup_{k=1}^{M} Q_k$, $\alpha_{k_0} = \min\{\alpha_1, ..., \alpha_M\}$, *and* $s > 0$.

6. **Numerical experiments.** In this section, we will compare the approximation quality of our proposed PHLST with adaptive tiling and that with the uniform tiling using three representative Antarctic remote sensing images. To approximate an image, PHLST first tiles an image into local blocks using the characteristic functions. The minimal size of each block of the PHLST algorithm is set to either 9×9 or 17×17 [11]. The quality of image approximation is measured by PSNR (peak signal-to-noise ratio) [6, 10]

$$\text{PSNR} := 20 \times \log_{10}\left(\max_{x\in\Omega} |f(x)|/\text{RMSE}\right),$$

where RMSE is the absolute ℓ^2 error between the original and the approximation divided by the square root of the total number of pixels in the original image. The unit of PSNR is decibel (dB).

The Erebus Ice Tongue (Figure 1, left) is a mountain outlet glacier that projects 11-12 km into McMurdo Sound from the Ross Island coastline near Cape Evans, Antarctica. It is about 10 meters high and is centered upon 77.6 degrees south latitude, 166.75 degrees east longitude. For the adaptive tiling, we first detect the points where the local Besov index attains the local minimum in Erebus Ice Tongue image. Here we do not need to compute exactly the value of local Besov index at each point. What we need is to find the location of points whose local Besov indices attain the local minima. From classic approximation theory [13, 7, 14], we know that the small local Besov indices correspond to the large pixel-value differences. Hence we use the popular Canny edge detector [3] to obtain these points by the output of the Canny edge detector (Figure 1,right). Using this information, we apply our adaptive tiling algorithm in Section 4 to the Erebus Ice Tongue image (Figure 2). Finally, we approximate this image by PHLST with uniform tiling and adaptive tiling. In Figure 3, we show the quality of approximation of Erebus Ice Tongue image when we retain 0.5%-5% of the original coefficients, measured by PSNR values. It is clear that we can better approximate images by PHLST with adaptive tiling than with uniform tiling. Finally, we show the reconstructed images

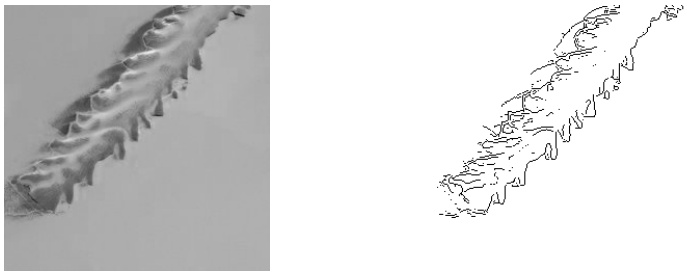

FIGURE 1. (Left) Erebus Ice Tongue image. (Right) The points where the local Besov indices attain the local minimal value in Erebus Ice Tongue image

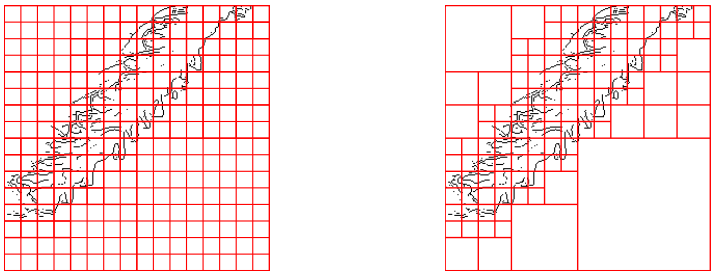

FIGURE 2. Uniform tiling and adaptive tiling of Erebus Ice Tongue image

because the PSNR plot does not tell the whole story. Figure 4 shows reconstructed images using the top 0.5 % of the coefficients by uniform tiling and adaptive tiling.

The next image we want to examine is that of Antarctica's McMurdo Sound (Figure 5), which is located bout 1,300 km from the South Pole. It was discovered by Captain James Clark Ross and named after Lt. Archibald McMurdo. The ice-clogged waters of Antarctica's McMurdo Sound extend about 55 km long and wide. The sound opens into the Ross Sea to the north. Figure 6 shows uniform tiling and adaptive tiling of the McMurdo Sound remote sensing image. Figure 7 shows the quality of approximation when we retain 0.5%-5% of the original coefficients.

The last image we want to examine is that of the Antarctic peninsula, which is experiencing extraordinary warming. Ice mass loss on the peninsula occurred at a rate of 60 billion tonnes in 2006. Several ice shelves along the Antarctic Peninsula have retreated or disintegrated in the last two decades. Figure 8 is a satellite image of a part of the Antarctic peninsula. Using uniform tiling and adaptive tiling in Figure 9, the quality of approximation is shown in Figure 10.

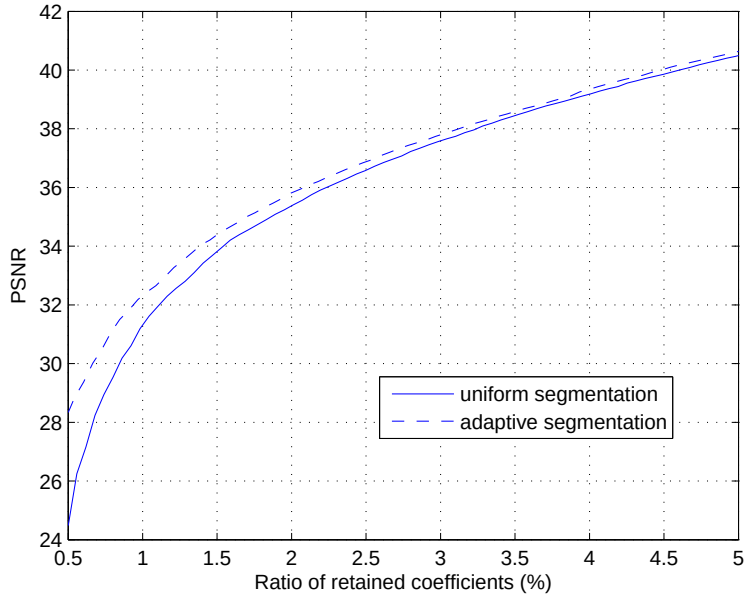

FIGURE 3. Quality of approximation of Erebus Ice Tongue image

(a) Original Image (b) Uniform Tiling (c) Adaptive Tiling

FIGURE 4. The reconstructed Erebus Ice Tongue images by using top 0.5% coefficients

7. **Conclusion.** In this paper, we proposed an efficient nonlinear image approximation scheme using PHLST combined with the automatic and adaptive tiling algorithm based on the local Besov indices of an input image. We demonstrated the importance of tiling an input image adaptively according to its regional smoothness and singularities for PHLST-based image approximation by comparing its performance with that of the uniform tiling using Antarctic remote sensing images, which often consists of a large smooth part and smaller singular regions representated by snow ripples, fractured ice, and coastlines.

Finally, we would like to mention that it is important to develop an efficient compression algorithm for a practical use of our approximation algorithm in such Antarctic remote sensing image analysis, which will involve efficient quantization

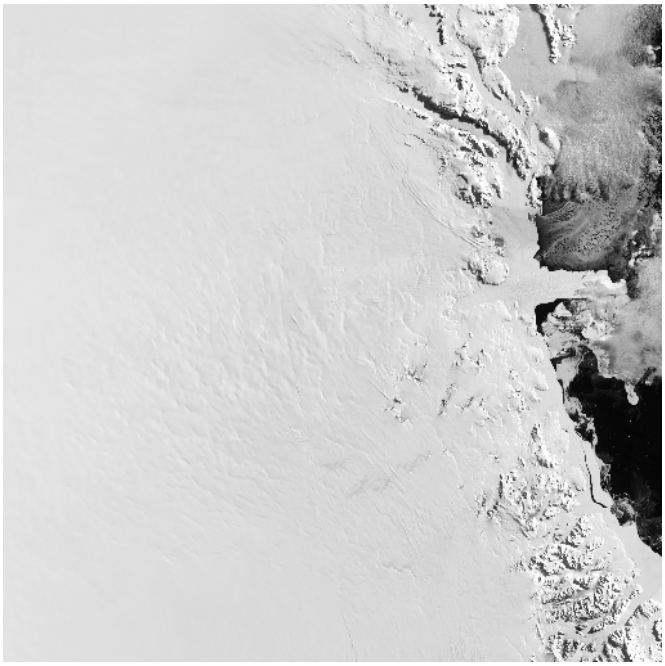

FIGURE 5. McMurdo Sound image

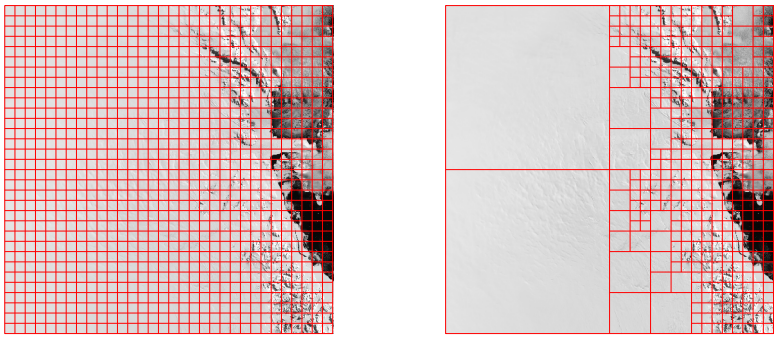

FIGURE 6. Uniform tiling and adaptive tiling of McMurdo Sound image

and entropy coding. We will pursue this direction and hope to report our results at a later date.

REFERENCES

[1] A. Averbuch, M. Israeli, and L. Vozovoi, *A fast Poisson solver of arbitrary order accuracy in rectangular regions*, SIAM J. Sci. Comput., **19** (1998), 933–952.

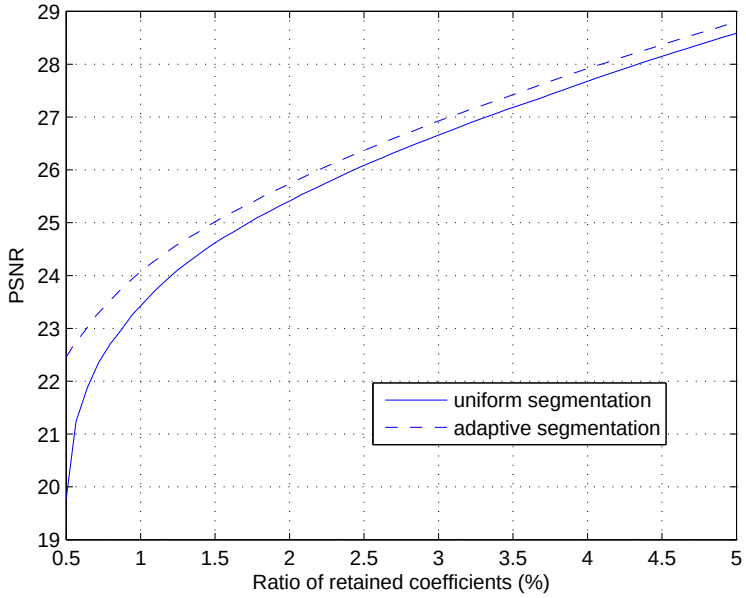

FIGURE 7. Quality of approximation of McMurdo Sound image

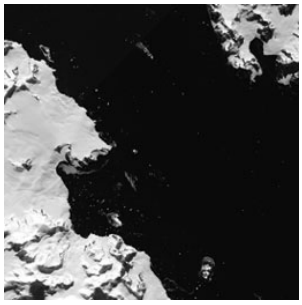

FIGURE 8. Satellite image of a part of the Antarctic peninsula

[2] E. Braverman, M. Israeli, A. Averbuch, and L. Vozovoi, *A fast 3D Poisson solver of arbitrary order accuracy*, J. Comput. Phys., **144** (1998), 109–136.
[3] J. F. Canny, *A computational approach to edge detection*, IEEE Trans. Pattern Anal. Machine Intell., **8** (1986), 679–698.
[4] R. A. DeVore and V. N. Temlyakov, *Nonlinear approximation by trigonometric sums*, J. Fourier Anal. Appl. **2** (1995), 29–48.
[5] R. R. Coifman and Y. Meyer, *Remarques sur l'analyse de Fourier à fenêtre,* Comptes Rendus Acad. Sci. Paris, Serie I, **312** (1991), 259–261.
[6] J. S. Lim, "Two-Dimensional Signal and Image Processing," Prentice Hall, Englewood Cliffs, NJ, 1990.
[7] G. G. Lorentz, "Approximation of Functions," 2nd Ed., Chelsea Pub. Co., New York, 1986.

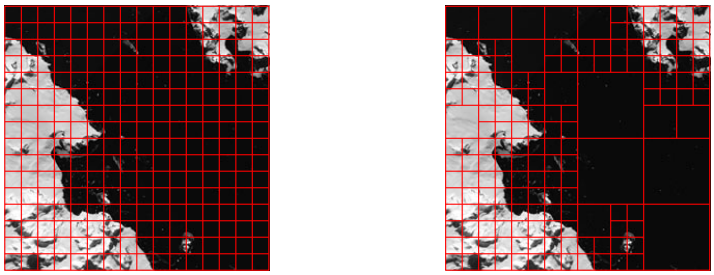

FIGURE 9. Uniform tiling and adaptive tiling of image of a part of the Antarctic peninsula

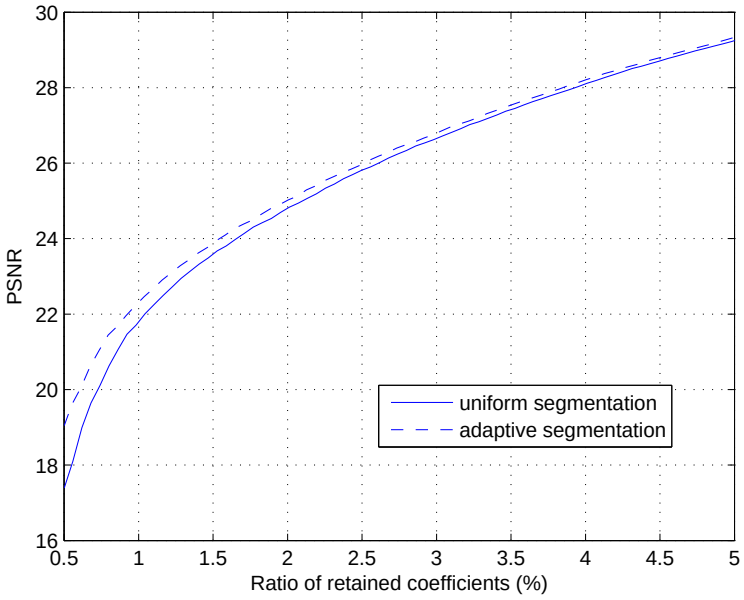

FIGURE 10. Quality of approximation of image of a part of the Antarctic peninsula

[8] H. S. Malvar, *Lapped transforms for efficient transform/subband coding,* IEEE Trans. Acoust., Speech, Signal Process., **38** (1990), 969–978.
[9] H. S. Malvar and D. H. Staelin, *The LOT: transform coding without blocking effects*, IEEE Trans. Acoust., Speech, Signal Process., **37** (1989), 553–559.
[10] J. R. Parker, "Algorithms for Image Processing and Computer Vision," John Wiley & Sons, Inc., New York, 1997.
[11] N. Saito and J.-F. Remy, *The polyharmonic local sine transform: A new tool for local image analysis and synthesis without edge effect*, Appl. Comput. Harmon. Anal. **20** (2006), 41–73.
[12] G. Strang, *The discrete cosine transform*, SIAM Review, **41** (1999), 135–147.
[13] A. F. Timan, "Theory of Approximation of Functions of a Real Variable," Macmillan, New York, 1963.

[14] A. Zygmund, "Trigonometric Series," 3rd Edition, Cambridge University Press, 2003.

Received xxxx 20xx; revised xxxx 20xx.

E-mail address: zhangzh@bnu.edu.cn
E-mail address: saito@math.ucdavis.edu